Journal of Quantitative Spectroscopy & Radiative Transfer 231 (2019) 1–8

Contents lists available at ScienceDirect

Journal of Quantitative Spectroscopy & Radiative Transfer

journal homepage: www.elsevier.com/locate/jqsrt

Self and N_2 collisional broadening of rovibrational lines in the ν_6 band of methyl iodide ($^{12}CH_3I$) at room temperature: The *J* and *K* dependence

Y. Attafi[a,b], A. Ben Hassen[b], H. Aroui[b], F. Kwabia Tchana[a,*], L. Manceron[c,d], D. Doizi[e], J. Vander Auwera[f], A. Perrin[g]

[a] *Laboratoire Interuniversitaire des Systèmes Atmosphériques (LISA), UMR CNRS 7583, Université Paris Est Créteil et Université Paris Diderot, Institut Pierre Simon Laplace, 61 avenue du Général de Gaulle, F-94010 Créteil Cedex, France*
[b] *Laboratoire de Spectroscopie et Dynamique Moléculaire, Université de Tunis, Ecole Nationale Supérieure d'Ingénieurs de Tunis, 5 Av Taha Hussein, 1008 Tunis, Tunisia*
[c] *Ligne AILES, Synchrotron SOLEIL, L'Orme des Merisiers, St-Aubin BP48, F-91192 Gif-sur-Yvette Cedex, France*
[d] *Sorbonne Université, CNRS, MONARIS, UMR 8233, 4 place Jussieu, F-75005 Paris, France*
[e] *DEN-Service d'Etude du Comportement des Radionucléides (SECR), CEA, Université Paris-Saclay, F-91191 Gif-sur-Yvette, France*
[f] *Service de Chimie Quantique et Photophysique, C.P. 160/09, Université Libre de Bruxelles, 50 avenue F.D. Roosevelt, B-1050 Brussels, Belgium*
[g] *Laboratoire de Météorologie Dynamique/IPSL, UMR CNRS 8539, Ecole Polytechnique, Université Paris-Saclay, RD36, F-91128 Palaiseau Cedex, France*

ARTICLE INFO

Article history:
Received 27 February 2019
Revised 12 April 2019
Accepted 12 April 2019
Available online 13 April 2019

Keywords:
Methyl iodide
CH3I
High-resolution Fourier transform spectroscopy
Self- and N2-broadening coefficients
J and K dependence

ABSTRACT

Following our recent study devoted to measurements of intensities of rovibrational lines in the ν_6 band of methyl iodide ($^{12}CH_3I$) centered at 892.918 cm^{-1}, room temperature infrared spectra of methyl iodide diluted in nitrogen at fourteen total pressures between 20 and 300 hPa have been recorded using the Fourier transform spectrometer Bruker IF125HR located at the LISA facility in Créteil. Three hundred and forty six N_2-broadening coefficients of methyl iodide rovibrational lines have been measured in the 824–951 cm^{-1} spectral range using mono-spectrum non-linear least squares fitting of Voigt profiles. Pressure-induced line shifts were not needed to fit the spectra to the noise level and line mixing effects could be neglected. Six hundred and eight self-broadening coefficients have also been measured in the same spectral range using the pure methyl iodide spectra recorded in our previous work. The measured self-broadening coefficients range from 0.1460 to 0.3786 cm^{-1} atm^{-1} and the N_2-broadening coefficients range from 0.0723 to 0.1481 cm^{-1} atm^{-1} at 295 K. The average accuracy on the measured self- and N_2-broadening coefficients was estimated to 3%. Comparisons with measurements reported in the literature for the ν_5 band of CH_3I shows a satisfactory agreement with average differences of 7% and 4% for the self- and N_2-broadening coefficients, respectively. The *J* and *K* rotational dependences of these coefficients have been observed and the latter modeled using an empirical polynomial expansion. On average, the empirical expression reproduces the measured self- and N_2-broadening coefficients to within 3% and 4%, respectively. The data obtained in the present work represent a significant contribution to the determination of broadening coefficients of CH_3I and complement the list of line positions and intensities generated in our previous work, thus providing useful spectroscopic information for atmospheric remote sensing and industrial detection of CH_3I.

1. Introduction

Remote sensing is a valuable tool for detecting and monitoring the composition of the Earth's atmosphere as well as for probing the molecular content of interstellar clouds or the atmospheres of solar and extra-solar objects [1–8]. The successful analysis of atmospheric and astrophysical spectra and the reliability of the retrieved concentrations and temperature profiles however strongly depend on the accuracy of available spectroscopic parameters, such as the positions, intensities, and pressure broadening and shifting coefficients of spectral lines. Spectroscopic information measured in the laboratory is collected into a number of databases, such as HITRAN [9] and GEISA [10], continuously updated in terms of accuracy of the line parameters, molecular species and spectral coverage.

* Corresponding author.
E-mail address: fridolin.kwabia@lisa.u-pec.fr (F.K. Tchana).

https://doi.org/10.1016/j.jqsrt.2019.04.017
0022-4073/

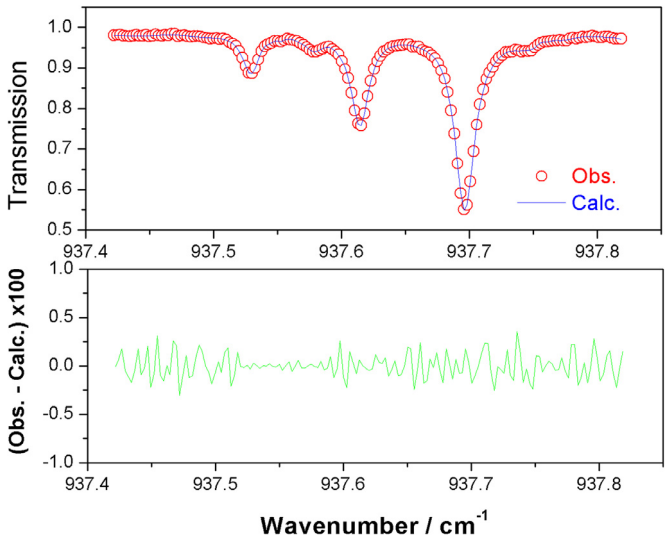

Fig. 1. The upper panel presents a small part of the spectrum of the ν_6 band of CH_3I perturbed by N_2 (spectrum 4 in Table 1; open circles) overlaid by the corresponding best-fit calculated spectrum (solid line) obtained with a source aperture diameter of 2 mm, a maximum optical path difference of 150 cm and a Voigt profile. The lower panel shows the percent differences between the observed and calculated spectra.

Table 1
Pressures of CH_3I and N_2 used to record the spectra. The numbers provided between parentheses are the uncertainties, estimated to be equal to 0.5% of the measured pressure. All the spectra correspond to the average of 1380 interferograms.

#	CH_3I pressure (hPa)	N_2 pressure (hPa)
S1	0.267 (1)	20.00 (10)
S2	0.333 (2)	33.33 (17)
S3	0.667 (3)	53.33 (27)
S4	0.835 (4)	67.42 (34)
S5	1.000 (5)	80.09 (40)
S6	1.169 (6)	93.37 (47)
S7	1.332 (7)	106.66 (53)
S8	1.667 (8)	132.86 (66)
S9	2.000 (10)	160.3 (8)
S10	2.333 (12)	186.9 (9)
S11	2.664 (13)	213.6 (1.1)
S12	3.001 (15)	240.2 (1.2)
S13	3.333 (17)	266.6 (1.3)
S14	3.665 (18)	293.3 (1.5)

Methyl iodide (CH_3I), the molecule of interest in the present work, is essentially absent from common spectroscopic databases, despite its atmospheric importance. Indeed, CH_3I is emitted in the atmosphere by marine algae and photolyzed with a lifetime of the order of a week. It is a source of I atoms involved in the ozone destruction cycles in the upper troposphere and in the lower stratosphere [11]. Methyl iodide is also of nuclear interest. In nuclear power plants, it is mainly produced in the containment by the reaction of iodine with organic coatings of the enclosure under ionizing radiation. In the case of a severe nuclear accident, iodine fission products represent the major part of the released radioactivity and are of high concern due to the affinity of iodine with the thyroid. It is therefore crucial to monitor the release of iodine compounds into the atmosphere, as part of the nuclear safety and radio-protection. To the best of our knowledge, there is up to now no infrared detection of these species in the atmosphere from a satellite instrument. The rather strong ν_6 band of CH_3I, located at 892.918 cm^{-1}, coinciding with the 11 µm transparency window in the atmosphere [12–14], could be a good candidate for such detection.

To prepare for this possible future detection, we recently carried out detailed studies concerning the line positions and intensities of the strong ν_6 band [15,16], which resulted in a list of line positions and intensities of CH_3I at 11 µm. This molecule was the subject of numerous microwave and infrared studies focused on the ground and various excited states, and several combination bands (see [15,16 and references therein] for an exhaustive review on the spectroscopic parameters of CH_3I). To the best of our knowledge, only two studies dealt with the measurement of line broadening coefficients [17,18]. Self-broadening parameters of 6 hyperfine components of the ($J = 10 \rightarrow 9$, $KI = 9$) rotational transitions in the $v_6 = 1$ excited vibrational state were accurately measured using Doppler-free double-resonance spectroscopy [17], and room temperature self-, N_2- and O_2-broadening coefficients were measured for over 100 lines in five Q-branches of the ν_5 perpendicular band at 7 µm using diode laser absorption spectroscopy [18].

The measurements reported here provide the first extensive data set that can be used for modeling pressure broadening coefficients of CH_3I. This work focuses on the self and N_2 collisional broadening of rovibrational lines in the ν_6 band of CH_3I at room temperature. The self-broadening coefficients have been measured using the pure methyl iodide spectra recorded in our previous work [16]. The N_2 collisional broadening coefficients were retrieved from fourteen high resolution Fourier transform spectra recorded at a temperature of 295 K. An empirical model was then developed to reproduce within experimental accuracy the large set of measured broadening coefficients covering various J and K values.

Section 2 details the experimental setup and conditions used to record the spectra. The measurements of self and N_2 broadening coefficients are described in Section 3. The empirical model developed to calculate self and N_2 collisional broadening parameters of CH_3I and comparisons of the present measurements with literature data are described in Section 4. Conclusions and remark are provided in Section 5.

2. Experimental details

Fourteen absorption spectra of methyl iodide diluted in nitrogen have been recorded in the range from 500 to 1450 cm^{-1} using the high-resolution Bruker IFS125HR FTS located at the LISA facility in Créteil (France). The instrument was equipped with a silicon carbide Globar source, a KBr/Ge beamsplitter and a liquid nitrogen cooled HgCdTe (MCT) detector. An optical filter with a bandpass of 500–1450 cm^{-1} was used to improve the signal-to-noise ratio. The FTS was continuously evacuated below 3×10^{-4} hPa by a turbomolecular pump to minimize absorption by atmospheric gases. The diameter of the entrance aperture of the spectrometer was set to 2 mm to maximize the intensity of infrared radiation falling onto the MCT detector without saturation or loss of spectral resolution. Interferograms were recorded with a 40 kHz scanner frequency and a maximum optical path difference (MOPD) of 150 cm. According to the Bruker definition (resolution = 0.9/MOPD), this corresponds to a resolution of 0.006 cm^{-1}.

The N_2 and CH_3I samples were purchased from Sigma Aldrich with stated purities of 99.99% and 99%, respectively. No further sample purifications were done. The absorption cell has a base path length of 20 cm and was adjusted for 28 transits in the present experiment, yielding an absorption path length of 564.9 ± 1.1 cm. The path length includes the distance between the surface of the field mirror and the windows of the cell (2×2.45 cm). The spectra were recorded at a stabilized room temperature of 295 ± 1 K. The sample pressure in the cell was measured using calibrated MKS Baratron capacitance manometers models 628D (2 and 10 Torr full scale) and 627D (100 and 1000 Torr full scale), characterized by a stated reading accuracy of

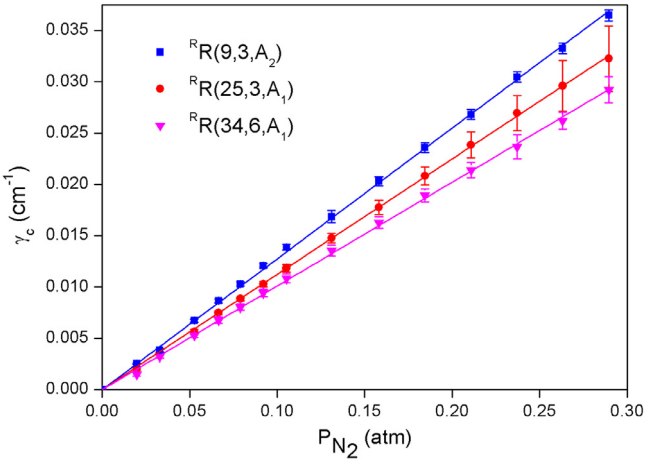

Fig. 2. Evolution with pressure of the N_2-collisional halfwidth of the $^{R}R(9,3,A_2)$, $^{R}R(25,3,A_1)$ and $^{R}R(34,6,A_1)$ lines in the ν_6 band of CH_3I perturbed by N_2. The slope of the best-fit lines represent the **N_2-broadening coefficients** γ_{N_2}. The displayed error bars are twice the uncertainties of measurement.

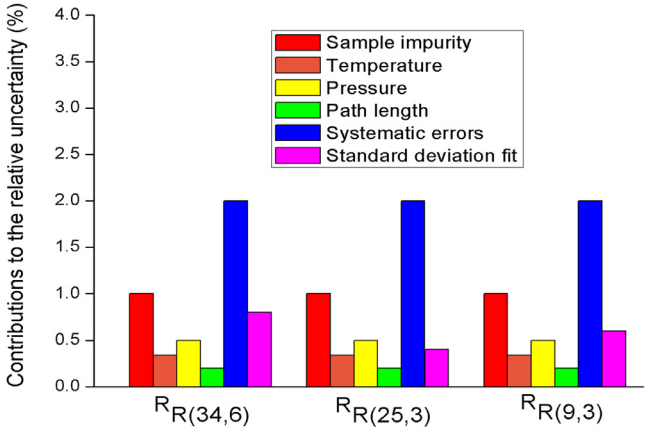

Fig. 3. Comparison between various sources of relative uncertainty on the measured N_2-broadening coefficients of 3 selected lines: $^{R}R(34,6)$, $^{R}R(25,3)$ and $^{R}R(9,3)$.

0.12%. Considering the uncertainty arising from small variations of the pressure during the recording of the interferograms (~0.35%), we estimated the measurement uncertainty on the pressure to be equal to 0.5%.

The following procedure was used for the measurements. A background spectrum was first recorded at a resolution of 0.01 cm^{-1} while the cell was being continuously evacuated. The cell was then filled with CH_3I at a given pressure, followed by the perturbing gas leading to a series of 14 total pressures. One CH_3I/N_2 spectrum was recorded for each CH_3I filling. Transmittance spectra were finally generated from the ratio of the sample spectra with the background spectrum. The fourteen pressures chosen and the number of interferograms recorded and averaged to yield the corresponding spectra are listed in Table 1. For the Fourier transform, a Mertz-phase correction with a 1 cm^{-1} phase resolution, a zero-filling factor of 2 and no apodization (boxcar option) were applied to the averaged interferograms. The root mean square (RMS) S/M in the ratioed spectra is around 300. The spectra were calibrated by matching the measured positions of about 30 lines of residual CO_2 observed therein to reference wavenumbers available in HITRAN2016 [9] with a RMS deviation of 0.00028 cm^{-1}.

3. Retrieval of the broadening coefficients and uncertainty analysis

3.1. Retrieval of self-broadening coefficients

The self-broadening parameters of rovibrational lines of methyl iodide were retrieved during our line intensities study, from simultaneous fits of the pure methyl iodide spectra recorded in our previous work [16] using a multi-spectrum least squares fitting algorithm, developed in Brussels [19,20]. This program adjusts spectroscopic (e.g. line positions, intensities and widths) and spectrum-specific (e.g. baseline) parameters to best-fit synthetic spectra to the observed spectra using a Levenberg–Marquardt non-linear least squares fitting procedure. Line intensities and self-broadening coefficients were retrieved simultaneously. The self-shift coefficients of all the lines were set to zero as signatures characteristic of self-shift were not be observed. Details on these measurements can be found in our previous work [16], in which the measured self-broadening coefficients were however not reported. We report 608 of these self-broadening coefficients in the present work, measured for lines having an absorption between 20 and 80%. As example, the results obtained for a few transitions are provided in Table 2. The whole set of measurements is given as supplementary material. The measured self-broadening coefficients range from 0.1460 to 0.3786 cm^{-1} atm^{-1} at 295 K.

3.2. Retrieval of nitrogen-broadening coefficients and uncertainty analysis

The CH_3I/N_2 collisional half widths were measured using a mono-spectrum non-linear least squares fitting program, already used and described in previous works [21–26]. Briefly, the measurements involved the adjustment of a calculated spectrum to the observed spectrum using a non-linear least squares fitting procedure. Each calculated spectrum was computed as the convolution of a Voigt-type transmission spectrum with an instrument line shape function, which included the effects of the finite maximum optical path difference and of the finite source aperture diameter of the interferometer [27]. In the present work, no deviation from this instrument line shape model was observed using the nominal aperture diameter of 2 mm. The background in each spectrum was represented by a polynomial expansion up to the second order (a constant or an affine function was however found sufficient in most cases), and the profile of the lines was modeled using a Voigt function with Gaussian width always held fixed to the value calculated for the Doppler broadening. Line mixing effects could be neglected. The measurements were carried out on small spectral intervals, ranging from 0.1 to 0.5 cm^{-1} and containing one to several lines. An example of the fitting procedure is shown in Fig. 1. The absence of signatures out of the spectral noise in the residuals suggests that the Voigt profile is adequate to fit the observed lines.

Although the spectra of the CH_3I/N_2 mixtures have been recorded with at most 1.3% of CH_3I, we subtracted the self-broadening contributions to deduce reliable N_2-broadening coefficients according to the equation:

$$\gamma_C = \gamma_{N_2} \times P_{N_2} = \gamma_{C,\ total} - \gamma_{self} \times P_{CH_3I} \quad (1)$$

where γ_c is the N_2-collisional halfwidth, $\gamma_{c,total}$ is the total collisional halfwidth, and P_{CH_3I} and P_{N_2} are the CH_3I and N_2 partial pressures, respectively. γ_{N_2} is the N_2-broadening coefficient and γ_{self} is the self-broadening coefficient. The evolution with the N_2 pressure of the N_2-collisional halfwidth γ_c measured for the $^{R}R(9,3,A_2)$, $^{R}R(25,3,A_1)$ and $^{R}R(34,6,A_1)$ lines of the ν_6 band of CH_3I is shown in Fig. 2. The fitted straight lines show the linear dependence of the collisional halfwidths with pressure. The N_2-broadening coefficients (in cm^{-1}atm^{-1}) can be derived from the slopes of these lines.

Table 2
Measured and calculated self- and N_2-broadening coefficients of few transitions of the ν_6 band of CH_3I. The whole set of measurements is provided as supplementary material.

(a)	(b)			(c)			(d)	(e)	(f)	(g)	(h)	(i)
839.24799	16	−4	E	17	−5	E	0.3579 ± 0.0101	0.3463	3.2	0.1234 ± 0.0037	0.1221	1.1
841.64068	39	−2	A2	40	3	A1	0.2484 ± 0.0062	0.2362	4.9	0.0985 ± 0.0029	0.1015	−3.0
844.96767	33	−2	A2	34	3	A1	0.2873 ± 0.0072	0.2841	1.1	0.1012 ± 0.0027	0.1036	−2.4
847.23064	30	−4	E	30	−5	E	0.3123 ± 0.0081	0.3103	0.6	0.0723 ± 0.0019	0.0717	0.9
849.25216	11	3	E	12	4	E	0.3133 ± 0.0079	0.3188	−1.8	0.1225 ± 0.0032	0.1200	2.0
852.33340	5	3	E	6	4	E	0.2434 ± 0.0071	0.2402	1.3	0.1144 ± 0.0033	0.1231	−7.6
854.52759	32	3	E	32	4	E	0.3036 ± 0.0077	0.2948	2.9	0.1059 ± 0.0033	0.1007	4.9
858.78192	7	−2	A1	8	3	A2	0.3046 ± 0.0077	0.2853	6.3	0.1238 ± 0.0033	0.1275	−3.0
861.22863	31	0	E	32	1	E	0.3220 ± 0.0082	0.2985	7.3	0.1164 ± 0.0029	0.1153	0.9
862.09850	30	−2	A2	30	3	A1	0.2913 ± 0.0072	0.3104	−6.6	0.0930 ± 0.0026	0.0907	2.5
865.81530	8	−1	E	9	−2	E	0.2974 ± 0.0077	0.2986	−0.4	0.1275 ± 0.0035	0.1262	1.0
872.50018	20	−2	A1	19	3	A2	0.3394 ± 0.0085	0.3489	−2.8	0.1122 ± 0.0027	0.1125	−0.3
876.28938	46	0	E	46	1	E	0.1867 ± 0.0053	0.2029	−8.7	0.1130 ± 0.0033	0.1078	4.6
881.11869	8	1	A1	9	0	A2	0.2915 ± 0.0074	0.3028	−3.9	0.1297 ± 0.0032	0.1280	1.3
884.06066	46	−2	A2	45	3	A1	0.2101 ± 0.0058	0.2035	3.1	0.1031 ± 0.0035	0.0993	3.7
889.47803	41	−1	E	40	−2	E	0.2470 ± 0.0064	0.2375	3.8	0.0983 ± 0.0026	0.1043	−6.1
894.03977	34	0	E	33	1	E	0.2866 ± 0.0073	0.2939	−2.5	0.1022 ± 0.0028	0.0992	2.9
897.07293	37	5	E	38	4	E	0.2567 ± 0.0074	0.2518	1.9	0.0972 ± 0.0027	0.0976	−0.4
899.19219	51	−3	E	51	−2	E	0.1502 ± 0.0040	0.1602	−6.7	0.0908 ± 0.0024	0.0935	−3.0
901.71089	17	2	E	16	1	E	0.3576 ± 0.0089	0.3518	1.6	0.1253 ± 0.0038	0.1198	4.4
903.77255	39	1	A2	38	0	A1	0.2570 ± 0.0065	0.2558	0.5	0.1100 ± 0.0031	0.1075	2.3
907.12091	47	1	A2	46	0	A1	0.2057 ± 0.0052	0.2037	1.0	0.1086 ± 0.0028	0.1084	0.2
911.25395	38	2	E	37	1	E	0.2532 ± 0.0064	0.2629	−3.8	0.0947 ± 0.0025	0.0973	−2.7
913.72387	26	−3	E	25	−2	E	0.3688 ± 0.0091	0.3493	5.3	0.1016 ± 0.0027	0.1114	−9.6
915.10727	47	2	E	46	1	E	0.1963 ± 0.0055	0.2029	−3.4	0.1027 ± 0.0026	0.1078	−5.0
917.43978	17	4	A2	16	3	A1	0.3484 ± 0.0086	0.3474	0.3	0.1112 ± 0.0031	0.1130	−1.6
921.66848	44	−3	E	43	−2	E	0.2012 ± 0.0053	0.2200	−9.3	0.1023 ± 0.0030	0.1036	−1.3
923.50244	13	5	E	12	4	E	0.3418 ± 0.0095	0.3188	6.7	0.1152 ± 0.0030	0.1200	−4.2
925.66545	35	4	A2	34	3	A1	0.2861 ± 0.0071	0.2841	0.7	0.1053 ± 0.0027	0.1036	1.6
929.11717	8	−6	E	7	−5	E	0.2574 ± 0.0065	0.2414	6.2	0.1179 ± 0.0031	0.1154	2.1
935.30843	21	−6	E	20	−5	E	0.3516 ± 0.0087	0.3538	−0.6	0.1092 ± 0.0030	0.1113	−1.9
939.62470	13	7	A2	12	6	A1	0.3085 ± 0.0076	0.3066	0.6	0.1219 ± 0.0034	0.1188	2.5
948.41621	32	7	A2	31	6	A1	0.3004 ± 0.0074	0.3029	−0.8	0.0820 ± 0.0023	0.0916	−11.7
949.74788	35	7	A2	34	6	A1	0.2798 ± 0.0069	0.2739	2.1	0.1010 ± 0.0025	0.0985	2.5
951.06367	38	7	A2	37	6	A1	0.2507 ± 0.0062	0.2510	−0.1	0.0932 ± 0.0026	0.0962	−3.2

(a) Line position (in cm^{-1}).
(b) Upper state quantum numbers J, $(K \times \ell)$ product, *Sym*. J and K are the rotational quantum numbers and *Sym* stands for A1, A2 and E symmetry. ℓ is the quantum number associated to the vibrational angular momentum.
(c) Lower state quantum numbers J, $(K \times \ell)$ product, *Sym*.
(d) Measured self-broadening coefficients (γ_{mea} in cm^{-1} atm^{-1}); uncertainties are calculated using Eq. (2).
(e) Self-broadening coefficients (γ_{calc} in cm^{-1} atm^{-1}) calculated using Eq. (3) and the values of the coefficients involved listed in Table 3.
(f) Differences $[(\gamma_{mea} - \gamma_{calc}) / \gamma_{mea}] \times 100$ between the measured γ_{mea} and calculated γ_{calc} self-broadening coefficients.
(g) Measured N_2-broadening coefficients (γ_{mea} in cm^{-1} atm^{-1}); uncertainties are calculated using Eq. (2).
(h) N_2-broadening coefficients (γ_{calc} in cm^{-1} atm^{-1}) calculated using Eq. (3) and the values of the coefficients involved listed in Table 3.
(i) Differences $[(\gamma_{mea} - \gamma_{calc}) / \gamma_{mea}] \times 100$ between the measured γ_{mea} and calculated γ_{calc} N_2-broadening coefficients.

Examination of the percent differences between the observed and best-fit calculated spectra (for example shown in the lower panel of Fig. 1) shows that they are generally less than 1%. However, estimation the accuracy of the measured broadening coefficients requires considering the uncertainties on all physical parameters, contributions from possible systematic errors [28] together with the standard deviation of the fits. These various sources of error and their associated uncertainties expressed relative to the broadening coefficients are given in Fig. 3 for 3 selected lines, representative of the 346 measured lines, i.e. $^{R}R(34,6)$, $^{R}R(25,3)$ and $^{R}R(9,3)$. Fig. 3 shows that systematic errors are the main sources of error. The dominant contributions to systematic errors arise from the location of the full-scale photometric level, channeling, as well as electronic and detector nonlinearities [28]. The reported estimate of 2% is an arbitrary, but conservative value. For each transition, we then estimated the accuracy of the 346 measured N_2-broadening coefficients from the uncertainties on the individual experimental parameters, i.e. ε_{si} (sample purity), ε_t (temperature), ε_p (pressure), ε_{pl} (pathlength), ε_{fit} (standard deviation from fit) and ε_{sys} (systematic errors), assuming that these uncertainties are uncorrelated:

$$\varepsilon = \sqrt{\varepsilon_{si}^2 + \varepsilon_t^2 + \varepsilon_p^2 + \varepsilon_{pl}^2 + \varepsilon_{fit}^2 + \varepsilon_{sys}^2} \quad (2)$$

On average, the estimated accuracy on the reported N_2-broadening coefficients is equal to 3%. In our analysis, we did not apply any temperature corrections to the measured broadening coefficients. Hence, the N_2-broadening coefficients listed in the supplementary material correspond to the temperature of 295 ± 1 K at which the spectra were recorded. The measured N_2-broadening coefficients range from 0.0723 to 0.1481 cm^{-1} atm^{-1} at 295 K. A few transitions are collected in Table 2, together with their absolute uncertainty.

4. Calculated self and N_2 collisional broadening parameters and discussion

4.1. Empirical model

We have fitted the measured self- and N_2-broadening coefficients to an empirical polynomial expression as previously done for

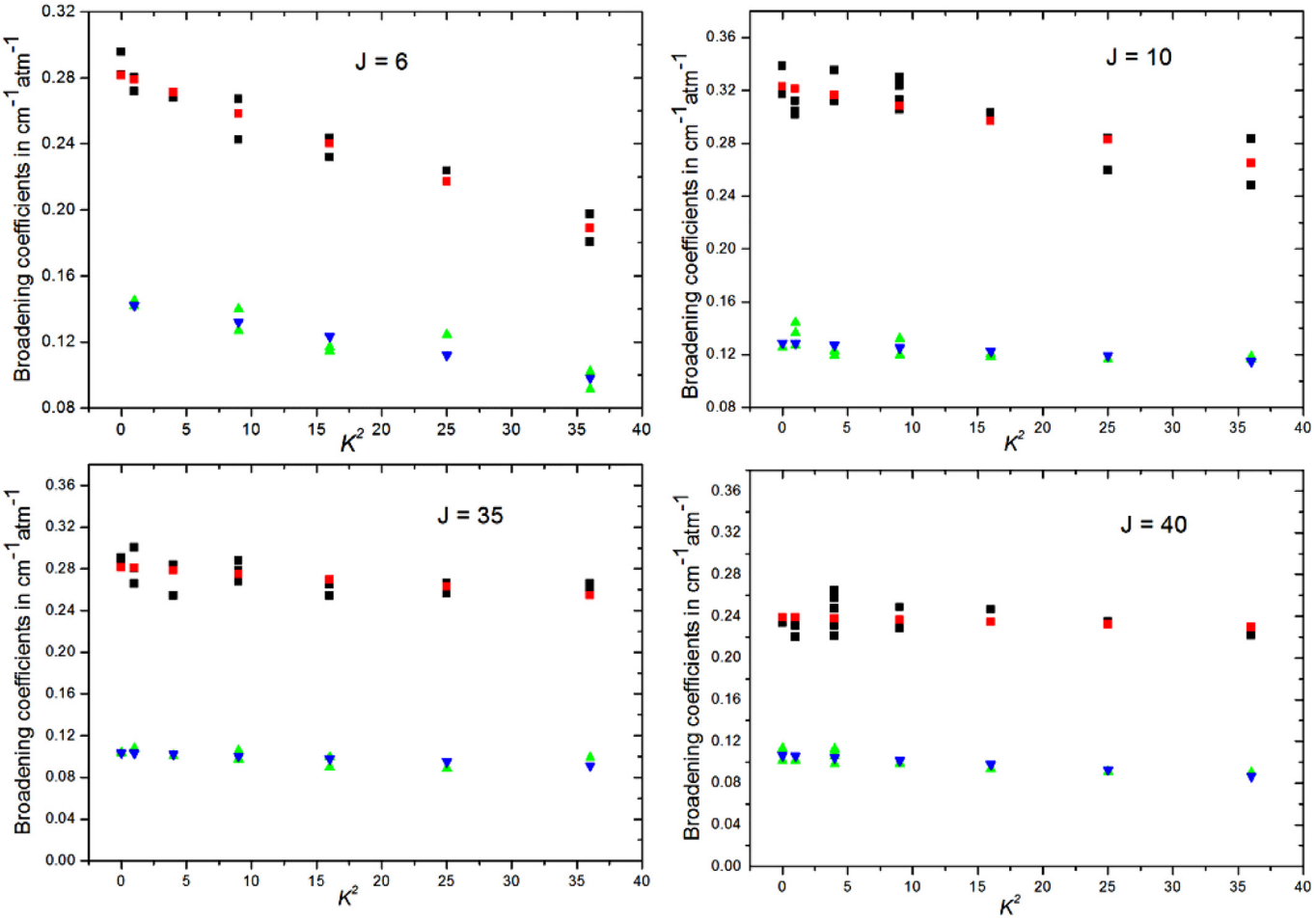

Fig. 4. Examples of fits to Eq. (3) of the self- and N_2-broadening coefficients for sets of measurements corresponding to $J=6$, 10, 35 and 40. The green up (▲) and blue down (▼) triangles are the measured and corresponding calculated N_2-broadening coefficients, respectively, and the black (■) and red (■) squares represent the measured and calculated self-broadening coefficients, respectively.

CH_3Br [25,29], CH_3F [30] and CH_3Cl [31–33]. Such a work requires a great amount of accurate measurements. For methyl iodide, this is the first time that an empirical model is used to adjust the measured broadening coefficients. Each set of broadening coefficients characterized by the same J value was fitted to the following polynomial expansion:

$$\gamma_J(K) = a_J^0 + a_J^2 K^2 \quad (3)$$

Examples of these fits are given in Fig. 4 for transitions with $J=6$, 10, 35 and 40. As has been observed in numerous studies dealing with C_{3v}-symmetry molecules [25,29–33], the broadening coefficients decrease with K. This decrease is more significant at low J than at high J values. The best-fit coefficients a_J^0 and a_J^2 were determined through a least-squares fit of the experimental broadening coefficients. They are listed in Table 3. The calculated self- and N_2-broadening coefficients (γ_{calc}) corresponding to the measured values (γ_{mea}) are presented in Table 2, together with the differences between the measured and calculated values. A statistical analysis of these differences (Table 4) shows that the fit is very good because at least 87% of the broadening coefficients fall within 7% of the measured values. On average, the empirical expression reproduces the measured self and N_2 broadening coefficients to within 3% and 4%, respectively. The latter range corresponds to the measurement uncertainty of the broadening coefficients. Figs. 5 and 6 are plots of the J-dependence of the self and N_2 broadening coefficients, respectively, measured and calculated for all studied K values in the ν_6 band of CH_3I. Fig. 5 shows that the self-broadening coefficients increase then decrease as J increases, exhibiting a maximum near $J=22$, while the N_2-broadening coefficients decrease with increasing J.

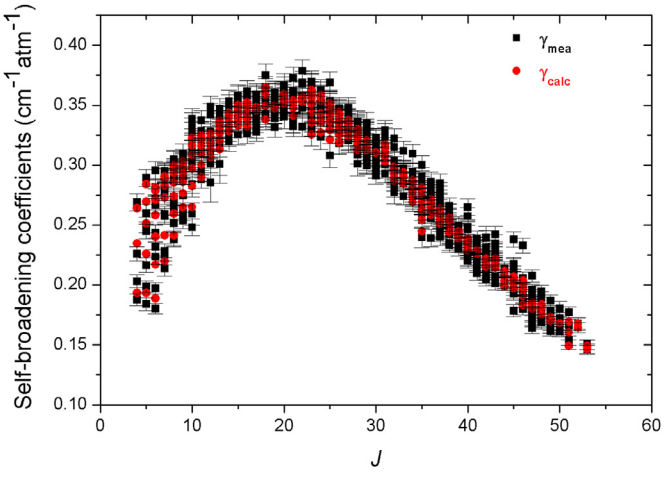

Fig. 5. J-dependence of the measured and calculated self-broadening coefficients for all studied K values in the ν_6 band of CH_3I.

Table 3
Best-fit coefficients a_J^2 and a_J^2 (in cm^{-1} atm^{-1}) involved in Eq. (3) used to reproduce the measured self- and N_2-broadening parameters of the ν_6 band of CH_3I.

J	Self a_J^0	a_J^2	N_2 a_J^0	a_J^2
4	0.2874(130)	−0.00587(105)	0.1656(101)	−0.00574(98)
5	0.2839(79)	−0.00362(49)	0.1372(71)	−0.00208(43)
6	0.2813(38)	−0.00257(21)	0.1432(43)	−0.00126(21)
7	0.2907(35)	−0.00197(20)	0.1313(30)	−0.00064(14)
8	0.2999(42)	−0.00162(22)	0.1335(42)	−0.00067(12)
9	0.3028(37)	−0.00105(22)	0.1280(21)	−0.00046(6)
10	0.3227(48)	−0.00160(29)	0.1287(24)	−0.00039(7)
11	0.3246(31)	−0.00097(18)	0.1251(34)	−0.00042(8)
12	0.3286(82)	−0.00061(11)	0.1209(34)	−0.000059(14)
13	0.3368(45)	−0.00065(12)	0.1175(33)	−0.00023(3)
14	0.3436(44)	−0.00042(7)	0.1197(37)	−0.00019(4)
15	0.3501(57)	−0.00048(9)	–	–
16	0.3524(33)	−0.00055(11)	0.1206(24)	−0.00084(14)
17	0.3482(45)	−0.000075(14)	0.1433(59)	−0.00085(12)
18	0.3699(67)	−0.00128(23)	0.1370(69)	−0.00154(27)
19	0.3494(39)	−0.000055(11)	0.1190(15)	−0.00072(14)
20	0.3591(43)	−0.00021(4)	0.1159(22)	−0.00018(4)
21	0.3540(45)	−0.00026(5)	0.1108(54)	−0.00116(18)
22	0.3565(48)	−0.00010(2)	0.1131(15)	−0.000079(12)
23	0.3626(34)	−0.00076(16)	0.1145(43)	−0.00054(7)
24	0.3594(18)	−0.00066(8)	0.1172(36)	−0.00035(7)
25	0.3518(42)	−0.00062(12)	0.1126(47)	−0.00029(5)
26	0.3438(22)	−0.00051(11)	0.1061(16)	−0.000076(10)
27	0.3375(29)	−0.00028(6)	0.1096(47)	−0.00011(2)
28	0.3297(41)	−0.00034(6)	0.1088(40)	−0.00020(4)
29	0.3203(40)	−0.00017(3)	0.1088(53)	−0.00055(8)
30	0.3105(53)	−0.0000054(11)	0.1014(35)	−0.00119(25)
31	0.3176(60)	−0.00041(8)	0.1107(79)	−0.00053(7)
32	0.2988(36)	−0.00025(5)	0.1163(38)	−0.00097(18)
33	0.2941(31)	−0.00020(4)	0.0997(23)	−0.00051(6)
34	0.2875(32)	−0.00038(8)	0.1053(17)	−0.00019(2)
35	0.2813(38)	−0.00075(15)	0.1033(20)	−0.00034(6)
36	0.2713(46)	−0.00036(7)	0.0964(53)	−0.00061(8)
37	0.2633(46)	−0.00034(6)	0.0973(18)	−0.000032(4)
38	0.2558(33)	−0.00025(4)	0.1075(23)	−0.00062(8)
39	0.2446(29)	−0.00016(3)	0.1012(49)	−0.00037(6)
40	0.2386(44)	−0.00026(4)	0.1065(21)	−0.00055(6)
41	0.2286(34)	−0.000078(14)	0.0935(36)	−0.000098(12)
42	0.2219(49)	−0.00019(4)	0.0932(42)	−0.00016(2)
43	0.2219(46)	−0.00046(8)	0.1062(39)	−0.00065(10)
44	0.2120(31)	−0.00054(10)	0.1063(54)	−0.00162(29)
45	0.2070(67)	−0.00039(7)	0.1014(17)	−0.0002(4)
46	0.2037(67)	−0.00082(15)	0.1084(30)	−0.00062(13)
47	0.1852(41)	−0.00014(2)	0.0938(34)	−0.00019(3)
48	0.1848(102)	−0.00107(23)	0.0977(38)	−0.00016(4)
49	0.1729(51)	−0.00018(4)	0.0911(27)	−0.00074(16)
50	0.1681(41)	−0.0000075(11)	0.0846(36)	−0.00046(6)
51	0.1690(65)	−0.00220(39)	0.1001(30)	−0.00164(26)
52	0.1676(2)	−0.00034(4)	–	–
53	0.1491(12)	−0.000077(14)	–	–

Note: Numbers between parentheses are the uncertainties (1 σ) in the units of the last quoted digit. For each J value, the number of broadening coefficients used in the fit ranges between 4 and 18 for the self-broadening coefficients and between 4 and 12 for N_2-broadening coefficients.

Table 4
Statistical analysis of the fit to Eq. (3) of the measured self and N_2 broadening coefficients of the ν_6 band of CH_3I ($\delta = |\gamma_{mea} - \gamma_{calc}| / \gamma_{mea} \times 100$).

	CH_3I broadener gas	N_2 broadener gas
Number of lines used in the fit	608	346
J_{max}	53	51
K_{max}	7	6
$0\% \le \delta < 4\%$	76%	55%
$4\% \le \delta < 8\%$	20%	32%
$8\% \le \delta < 15\%$	4%	13%

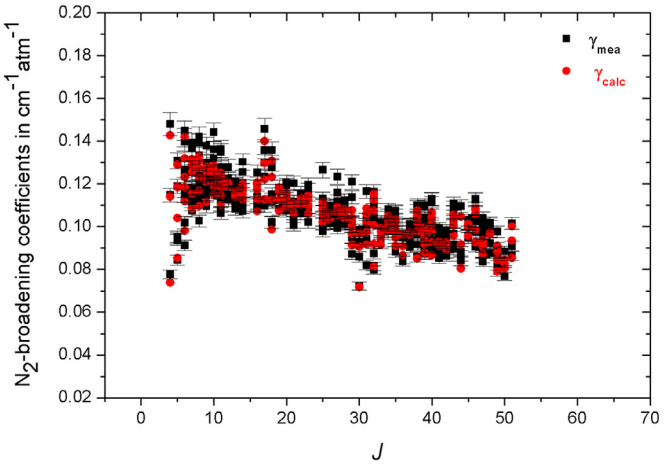

Fig. 6. J-dependence of the measured and calculated N_2-broadening coefficients for all studied K values in the ν_6 band of CH_3I.

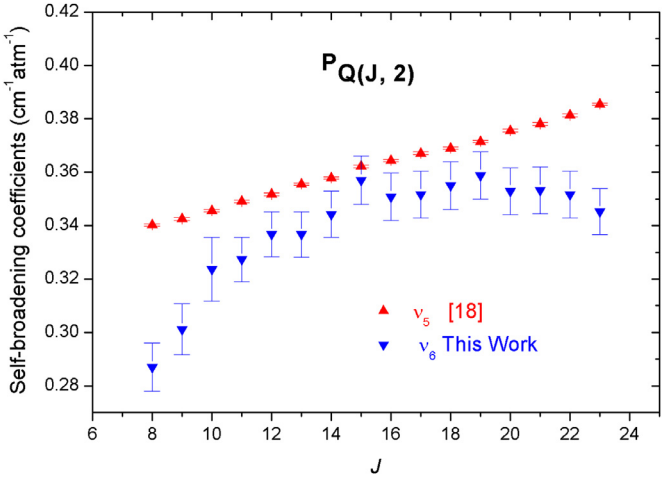

Fig. 7. Comparison of room temperature self-broadening coefficients measured in this work for $^PQ(J, 2)$ transitions in the ν_6 band of CH_3I with results reported by Hoffman and Davies [18] for the ν_5 band.

4.2. Comparison with previous work

In our previous study on line positions [15], the hyperfine structure had to be accounted for during the analysis and energy level calculation. For the line intensity measurements, we had carefully selected the transitions for which the hyperfine structure is not observable: this means that the hyperfine splitting is smaller than the Doppler line width [16]. In the present work, the experimental conditions do not allow differentiating the hyperfine components. Therefore, we did not compare our self-broadening coefficients with those of Belli et al. [17]. We therefore compared the self-broadening coefficients measured in this work with the only data available in the literature, i.e. the self-broadening coefficients reported for the ν_5 fundamental band of CH_3I [18]. Fig. 7 compares the present results for the $^PQ(J, 2)$ transitions in the ν_6 band and the measurements reported in Ref. [18] for the same transitions in the ν_5 band. The self-broadening coefficients reported for the ν_5 band are larger (the average difference is about 7%) and their rotational dependence is different. A similar comparison of N_2-broadening coefficients (Fig. 8) shows an overall good agreement with the results of Ref. [18], with an average difference of about 4%. The latter comparison tend to indicate the absence of a vibrational dependence of the N_2 broadening coefficients, similarly to what was observed for CH_3X (X = Br, F) [25,29,30].

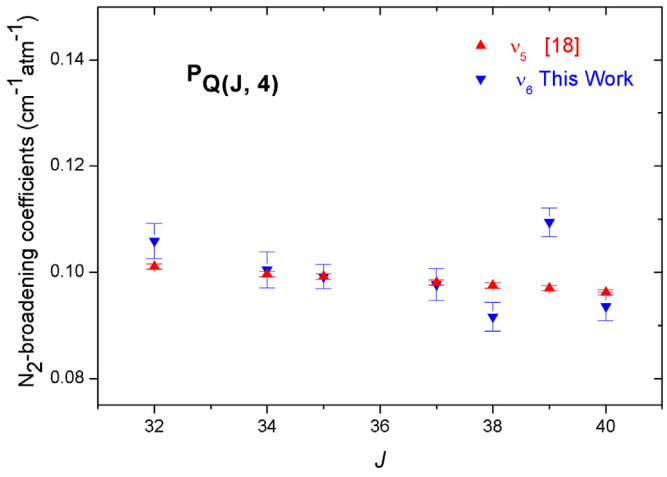

Fig. 8. Comparison of room temperature N_2-broadening coefficients measured in this work for $^{P}Q(J, 4)$ transitions in the ν_6 band of CH_3I with results obtained by Hoffman and Davies [18] for the ν_5 band.

5. Conclusion

Mono-spectrum analyses of high-resolution Fourier transform spectra of methyl iodide diluted in nitrogen at total pressures in the range 20–300 hPa resulted in the determination of N_2-broadening coefficients for rovibrational lines in the ν_6 band of methyl iodide, at room temperature. Self-broadening coefficients have also been measured at room temperature using multi-spectrum analyses of high-resolution Fourier transform spectra of pure methyl iodide recorded in one of our previous work [16]. Pressure-induced line shifts were not needed to fit the spectra down to the noise level in the multi-spectrum analysis carried out in Ref. [16] and line mixing effects could be neglected in both analyses. Self and N_2 broadening coefficients have been obtained for large sets of J and K values, for which clear J and K dependences have been observed. The N_2 broadening coefficients measured in the present work agree well with measurements reported in the literature for the ν_5 band of methyl iodide, while some discrepancies are observed for the self-broadening coefficients. Empirical polynomial expression have been used to model the rotational K dependence of the broadening coefficients, leading to accurate coefficients (a_J^0 and a_J^2) for methyl iodide. The measured and calculated self and N_2 broadening coefficients obtained in the present work and in Ref. [16] are provided as supplementary material, together with the assignment of the corresponding transitions. The data obtained in the present work represent a significant contribution to the determination of broadening coefficients of methyl iodide and thus completes the list of line positions and intensities generated in our previous work [16], useful for atmospheric remote sensing and industrial detection of methyl iodide. It will be necessary to complete them with experimental determination of broadening coefficients at temperatures observed in the Earth's atmosphere.

Acknowledgments

The DECA-PF project is sponsored by the French government 'Investments for the future' program through the grant ANR-11-RSNR-0003 supervised by the French National Research Agency (ANR) under the 'Research in Nuclear Safety and Radioprotection' (RSNR) research initiative.

Supplementary materials

Supplementary material associated with this article can be found, in the online version, at doi:10.1016/j.jqsrt.2019.04.017.

References

[1] Demaison J, Sarka K, Cohen EA. Spectroscopy from space. Spectroscopy from space. Dordrecht: Kluwer Academic Publisher; 2001.
[2] Niro F, Hase F, Camy-Peyret C, Payan S, Hartmann JM. Spectra calculations in central and wing regions of CO_2 IR bands between 10 and 20 µm. II: atmospheric solar occultation spectra. J Quant Spectrosc Radiat Transf 2005;90:43–59.
[3] Hay KG, Wright S, Duxbury G, Langford N. In-flight measurements of ambient methane, nitrous oxide and water using a quantum cascade laser based spectrometer. Appl Phys B 2008;90:329–37.
[4] Duxbury G, Langford N, Hay K, Tasinato N. Quantum cascade laser spectroscopy: diagnostics to non-linear optics. J Mod Opt 2009;56:2034–48.
[5] McNaughton D, Robertson EG, Thompson CD, Chimdi T, Bane MK, Appadoo D. Overview of high-resolution infrared measurement and analysis for atmospheric monitoring of halocarbons. Anal Chem 2010;82:7958–64.
[6] Brown AT, Chipperfield MP, Boone C, Wilson C, Walker KA, Bernath PF. Trends in atmospheric halogen containing gases since 2004. J Quant Spectrosc Radiat Transf 2011;112:2552–66.
[7] Swain MR, Vasisht G, Tinetti G. The presence of methane in the atmosphere of an extrasolar planet. Nature 2008;452:329–31.
[8] Tinetti G, Vidal-Madjar A, Liang MC, Beaulieu JP, Yung Y, Carey S, et al. Water vapour in the atmosphere of a transiting extrasolar planet. Nature 2007;448:169–71.
[9] Gordon IE, Rothman LS, Hill C, Kochanov RV, Tana Y, Bernath PF, Birk M, Boudon V, Campargue A, Chance KV, Drouin BJ, Flaud JM, Gamache RR, Hodges JT, Jacquemart D, Perevalov VI, Perrin A, Shine KP, Smith MA, Tennyson J, Toon GC, Tran H, Tyuterev VG, Barbe A, Császár AG, Devi VM, Furtenbacher T, Harrison JJ, Hartmann JM, Jolly A, Johnson TJ, Karman T, Kleiner I, Kyuberis AA, Loos J, Lyulin OM, Massie ST, Mikhailenko SN, Moazzen-Ahmadi N, Müller HSP, Naumenko OV, Nikitin AV, Polyansky OL, Rey M, Rotger M, Sharpe SW, Sung K, Starikova E, Tashkun SA, Vander Auwera J, Wagner G, Wilzewski J, Wcisło P, Yuh S, Zak EJ. The HITRAN 2016 molecular spectroscopic database. J Quant Spectrosc Radiat Transf 2017;203:3–69.
[10] Jacquinet-Husson N, Armante R, Scott NA, Chédin A, Crépeau L, Boutammine C, Bouhdaoui A, Crevoisier C, Capelle V, Boonne C, Poulet-Crovisier N, Barbe A, Benner DC, Boudon V, Brown LR, Buldyreva J, Campargue A, Coudert LH, Devi VM, Down MJ, Drouin BJ, Fayt A, Fittschen C, Flaud JM, Gamache RR, Harrison JJ, Hill C, Hodnebrog Ø, Hu SM, Jacquemart D, Jolly A, Jiménez E, Lavrentieva N, Liu AW, Lodi L, Lyulin OM, Massie ST, Mikhailenko S, Müller HSP, Naumenko OV, Nikitin A, Nielsen CJ, Orphal J, Perevalov V, Perrin A, Polovtseva E, Predoi-Cross A, Rotger M, Ruth AA, Shanshan Y, Sung K, Tashkun S, Tennyson J, Tyuterev VG, Vander Auwera J, Voronin B, Makie A. The 2009 edition of the GEISA spectroscopic database. J Mol Spectrosc 2016;327:31–72.
[11] Bell N, Hsu L, Jacob DJ, Schultz MG, Blake DR, Butler JH, King DB, Lobert JM, Maier-Reimer E. Methyl iodide: atmospheric budget and use as a tracer of marine convection in global models. J Geophys Res 2002;107(D17):4340.
[12] Bernath P. Atmospheric chemistry experiment: spectroscopy from orbit. Opt Photonics News 2005;16(4):24–7.
[13] Fischer H. The MIPAS experiment aboard ENVISAT: remote sensing of atmospheric composition. In: Perrin A, Ben Sari-Zizi N, Demaison J, editors. Remote sensing of the atmosphere for environmental security. Dordrecht: Springer; 2006. p. 41–55.
[14] Clerbaux C, Boynard A, Clarisse L, George M, Hadji-Lazaro J, Herbin H, et al. Monitoring of atmospheric composition using the thermal infrared IASI/MetOp sounder. Atmos Chem Phys 2009;9:6041–54.
[15] Perrin A, Haykal I, Kwabia-Tchana F, Manceron L, Doizi D, Ducros G. New analysis of the ν_6 and $2\nu_3$ bands of methyl iodide (CH_3I). J Mol Spectrosc 2016;324:28–35.
[16] Kwabia Tchana F, Attafi Y, Manceron L, Doizi D, Vander Auwera J, Perrin A. Line intensities for the ν_6 and $2\nu_3$ bands of methyl iodide ($^{12}CH_3I$). J Quant Spectrosc Radiat Transf 2019;222-223:130–7.
[17] Belli S, Buffa G, Di Lieto A, Minguzzi P, Tarrini O, Tonelli M. Hyperfine level dependence of the pressure broadening of CH_3I rotational transitions in the $v_6 = 1$ vibrational state. J Mol Spectrosc 2000;201:314–18.
[18] Hoffman KJ, Davies PB. Pressure broadening coefficients of ν_5 fundamental band lines of CH_3I at 7µm measured by diode laser absorption spectroscopy. J Mol Spectrosc 2008;252:101–7.
[19] Tudorie M, Foldes T, Vandaele AC, Vander Auwera J. CO_2 pressure broadening and shift coefficients for the 1-0 band of HCl and DCl. J Quant Spectrosc Radiat Transf 2012;113:1092–101.
[20] Daneshvar L, Foldes T, Buldyreva J, Vander Auwera J. Infrared absorption by pure CO_2 near 3340 cm^{-1}: measurements and analysis of collisional coefficients and line-mixing effects at subatmospheric pressures. J Quant Spectrosc Radiat Transf 2014;149:258–74.
[21] Kwabia Tchana F, Jacquemart D, Lacome N, Kleiner I, Orphal J. Absolute line intensities in methyl bromide: the 7-µm region. J Mol Spectrosc 2006;235:132–43.

[22] Kwabia Tchana F, Ngom M, Perrin A, Flaud JM, Lafferty WJ, Ndiaye SA, Ngom El A. Absolute line intensities for oxirane from 1420 to 1560 cm^{-1}. J Mol Spectrosc 2013;292:1–4.
[23] Ngom M, Flaud JM, Kwabia Tchana F, Lafferty WJ, Landsheere X, Perrin A, Ngom El A. Absolute line intensities for the ν_3 band of oxirane (C_2H_4O). Can J Phys 2013;91(11):906–9.
[24] Kwabia Tchana F, Flaud JM, Lafferty WJ. Ngom. Absolute line intensities for oxirane in the 11.4 μm spectral region. Mol Phys 2014;112:1633–8.
[25] Boussetta Z, Kwabia Tchana F, Aroui H. Self- and N_2-broadening of CH_3Br ro-vibrational lines in the ν_2 band: the J and K dependence. J Mol Spectrosc 2015;309(308):33–40.
[26] Ben Hassen A, Galalou S, Kwabia Tchana F, Dhib M, Aroui H. Self-and N_2-collisional broadening coefficients of ethylene in the 1800–2350 cm^{-1} spectral region. J Mol Spectrosc 2016;326:73–80.
[27] Dana V, Mandin JY. New improvements in the determination of line parameters from FTS data. J Quant Spectrosc Radiat Transf 1992;48(5–6):725–31.
[28] Ballard J, Knight RJ, Vander Auwera J, Herman M, Di Lonardo G, Masciarelli G, Nicolaisen FM, Beukes JA, Christensen LK, McPheat R, Duxbury G, Freckleton R, Shine KP. An intercomparison of laboratory measurements of absorption cross-sections and integrated absorption intensities for HCFC-22. J Quant Spectrosc Radiat Transf 2000;66:109–28.
[29] Jacquemart D, Kwabia Tchana F, Lacome N, Kleiner I. A complete set of line parameters for CH_3Br in the 10-μm spectral region. J Quant Spectrosc Radiat Transf 2007;105:264–302.
[30] Jacquemart D, Guinet M. Line parameters measurements and modeling for the ν_6 band of CH_3F: generation of a complete line list for atmospheric databases. J Quant Spectrosc Radiat Transf 2016;185:58–69.
[31] Barbouchi Ramchani A, Jacquemart D, Dhib M, Aroui H. Line positions, intensities and self-broadening coefficients for the ν_5 band of methyl chloride. J Quant Spectrosc Radiat Transf 2013;120:1–15.
[32] Bray C, Jacquemart D, Lacome N, Guinet M, Cuisset A, Eliet S, Hindle F, Mouret G, Rohart F, Buldyreva J. Self-broadening coefficients of methyl chloride transitions at room temperature. J Quant Spectrosc Radiat Transf 2013;116:88–100.
[33] Barbouchi Ramchani A, Jacquemart D. Line intensities and self-broadening coefficients for the ν_2 band of methyl chloride. J Mol Spectrosc 2016;326:81–6.